

Internal Friction Behavior of $Ti_{48}Zr_{20}Nb_{12}Cu_5Be_{15}$ Metallic Glass Composite

Cui Jing¹, Liu Yi², Liu Shu¹

¹ Industrial Training Centre, Shenzhen Polytechnic, Shenzhen 518055, China; ² School of Materials Science and Engineering, Luoyang Institute of Science and Technology, Luoyang 471023, China

Abstract: The mechanical properties at room temperature and the dynamic mechanical properties at different temperatures of $Ti_{48}Zr_{20}Nb_{12}Cu_5Be_{15}$ metallic glass composite were investigated. Results show that the tensile strength at room temperature of this metallic glass composite is about 1350 MPa and its fracture strain is approximately 0.13. With increasing the temperature, the state of the metallic glass composite changes from elastic to viscoelastic. The physical parameters, such as loss factor and correlation coefficient, are introduced to analyze the dynamic mechanical behavior under the framework of quasi-point defects model, and the theoretical curve fits well with the experiment data. Therefore, the quasi-point defects model can well describe the dynamic mechanical behavior of $Ti_{48}Zr_{20}Nb_{12}Cu_5Be_{15}$ bulk metallic glass composite at different temperatures.

Key words: metallic glass composite; mechanical property; dynamic mechanical behavior; quasi-point defects

Benefitting from the long/short-range disordered atomic configurations and absence of the defects in conventional alloys (grain boundary, dislocation), bulk metallic glasses (BMGs) show excellent mechanical properties, such as high hardness, large elastic area, and outstanding formability^[1-6]. But the room-temperature brittleness restricts their applications as structural material in commercial proliferation^[7]. It is known that the metallic glass is homogeneous and isotropic, so its plasticity or ductility depends on the rearrangements of atoms in some weak areas, such as shear transformation zone (STZ)^[8-12], free volume^[13], or flow unit^[12,14-17]. When an external stress is applied on metallic glass, the atoms in these weak areas will move to the near vacancies. Therefore, the flow of these weak areas leads to the formation of nano-size shear bands^[10,18,19]. The shear band is a typical characteristic of plasticity behavior, and the number of shear bands is very limited during the deformation^[20]. Thus, the unhindered propagation of the limited shear bands causes the catastrophic fracture of the metallic glass^[21-24].

Consequently, many efforts have been devoted to ameliorate the ductility of BMGs, especially their tensile

plasticity. The methods include optimizing specimen shape^[25,26], synthesizing new BMG^[27,28], reducing specimen size^[29], and adding the secondary phase^[30]. During the optimization of specimen shape, some stress concentration points are prearranged on the specimen for initiation of shear bands with nano-sized thickness when the external stress is applied. Subsequently, the shear bands cross each other and the propagation is obstructed. Hence, more shear bands are formed and the plasticity of the specimen is improved. However, the application of this method is restricted because it can only be used for specific shapes, and cannot improve the plasticity of metallic glass. Synthesizing new metallic glass can significantly ameliorate the compressive plasticity but not the tensile ductility at the cost of strength. By reducing the specimen size to nanoscale which is smaller than the thickness of shear bands, the metallic glass can avoid the generation of shear bands and show tensile ductility and necking phenomenon. However, this method leads to the function failure of metallic glass for structural applications due to the absence of specimen-size effect. Among these methods, adding the secondary phases as reinforcement into amorphous matrix is more effective to form bulk metallic

Received date: May 24, 2021

Foundation item: Foundation for Young Talents of Shenzhen Polytechnic (601822K35018); Foundation for Young Talents in Higher Education of Guangdong (601821K35055); National Natural Science Foundation of China (51801026)

Corresponding author: Liu Shu, Ph. D., Industrial Training Centre, Shenzhen Polytechnic, Shenzhen 518055, P. R. China, E-mail: liushu814194678@szpt.edu.cn

Copyright © 2022, Northwest Institute for Nonferrous Metal Research. Published by Science Press. All rights reserved.

glass composites (BMGCs) with improved plasticity. The metallic glass composites can be divided into ex-situ metallic glass composites and in-situ metallic glass composites. To obtain the ex-situ metallic glass composites, some hard brittle or soft ductile particles should be added into the metallic glass matrix to form the reinforced secondary phases. Once the size of the reinforced secondary phases is larger than the thickness of shear bands, the propagation of shear bands is hindered. Then the tensile plasticity and fracture toughness of metallic glass composites at room temperature can be improved^[31-33]. However, the bonding between the reinforcement particles and metallic glass matrix can only improve the compressive plasticity but not the tensile ductility of metallic glass composites. There are many stress concentration points on the boundary between the reinforcement particles and metallic glass matrix, which can reduce the strength of metallic glass composites.

Due to different preparation methods, the in-situ metallic glass composites have perfect chemical bonding between the crystalline phases and metallic glass matrix. Adding pre-designed β -phase stable elements can promote the formation of some β -stabilizer dendrites during the solidification of metallic glasses. Subsequently, the in-situ metallic glass composites with metallic glass matrix and the secondary phases (B2 phases or β -stabilizer dendrites) can be obtained^[19,34-37]. Consequently, both the compressive and tensile plasticity of the material are improved without strength reduction. Moreover, the morphology and volume fraction of the secondary phase dendrites can be controlled by adjusting the composition of in-situ metallic glass composite, so the mechanical properties, tribological properties, or dynamic mechanical properties can be changed to meet various demands.

In this research, the in-situ Ti-based BMGC $\text{Ti}_{48}\text{Zr}_{20}\text{Nb}_{12}\text{Cu}_5\text{Be}_{15}$ (at%) with light weight and high strength was used to investigate the mechanical relaxation behavior under continuous heating. Because the composite matrix is amorphous, the quasi-point defect model was proposed to analyze the experiment results for study of physical properties.

1 Experiment

The alloy ingot with the nominal composition of $\text{Ti}_{48}\text{Zr}_{20}\text{Nb}_{12}\text{Cu}_5\text{Be}_{15}$ was prepared by arc-melting. The mixture of high purity elements (the purities of elements Ti, Zr, Nb, Cu, and Be are over 99.95%) was placed in a water-cooled copper crucible and the in-situ suction casting was conducted in a copper mold under the purified argon atmosphere. The alloy ingot was re-melted several times before suction casting to ensure the homogeneity. Then BMGC plates with the dimension of 50 mm×30 mm×3 mm were fabricated.

The nature phase of $\text{Ti}_{48}\text{Zr}_{20}\text{Nb}_{12}\text{Cu}_5\text{Be}_{15}$ BMGC specimen was identified by X-ray diffraction (XRD) with a diffractometer ($2\theta=20^\circ\sim 80^\circ$) using monochromatic Cu K α radiation (Philips X'Pert Pro). The working condition was 40 kV and 30 mA for the X-ray tube and the scanning rate was 0.02° per step. The thermal properties such as glass transition

temperature T_g and onset crystallization temperature T_x of BMGC were determined by differential scanning calorimetry (DSC, NETZSCH STA 449C) with a heating rate of 20 K/min under argon atmosphere. The microstructural features of as-cast BMGC were observed by scanning electron microscope (SEM, EVO 18, Zeiss, Germany). The specimens were etched by an etchant (volume ratio of HNO_3 : HF: ethanal=1: 1: 8) before the microstructure observation.

The mechanical property of $\text{Ti}_{48}\text{Zr}_{20}\text{Nb}_{12}\text{Cu}_5\text{Be}_{15}$ BMGC was studied through the uniaxial tensile tests at room temperature under the strain rate of $1.0\times 10^{-3}\text{ s}^{-1}$. The specimens with 10 mm in gage length, 2 mm in width, and 3 mm in thickness and the surfaces were carefully polished.

The dynamic mechanical behavior of the Ti-based BMGC was investigated using mechanical spectrometer^[38], namely dynamic mechanical analysis (DMA) in an inverted torsion mode. During DMA, the corresponding stress of the applied periodic stress was measured: the complex modulus ($G^*=G'+iG''$) was recorded with the storage dynamic shear modulus (G') and the loss dynamic shear modulus (G''). The loss factor (internal friction) can also be obtained as $\tan\delta=G''/G'$, which corresponds to loss energy in a cycle^[39]. The current experiments were conducted using a sinusoidal stress under two conditions: a fixed frequency from 10^{-4} Hz to 2 Hz during the continuous heating with a constant heating rate, and a given temperature with different frequencies. The Ti-based BMGC specimens with the dimension of 30 mm×2 mm×1 mm were prepared by precision cutting machine, and all the experiments were conducted in a high vacuum atmosphere. The strain amplitude was lower than 10^{-4} .

2 Results and Discussion

2.1 Microstructure, phase, and thermal analysis of as-cast BMGC

The phase components, microstructure, and thermal parameters of the as-cast BMGC were confirmed by XRD, SEM, and DSC. Fig.1a shows the phase constitution of the as-cast $\text{Ti}_{48}\text{Zr}_{20}\text{Nb}_{12}\text{Cu}_5\text{Be}_{15}$ BMGC. Three sharp crystalline peaks are identified as the characteristic peaks of β -Ti phase, indicating that $\text{Ti}_{48}\text{Zr}_{20}\text{Nb}_{12}\text{Cu}_5\text{Be}_{15}$ BMGCs are composed of β -Ti and amorphous phases. SEM image of BMGC is shown in Fig.1b. It can be seen that there are only two phases in BMGC and the secondary phase dendrites (β -Ti phase) are distributed evenly in the glassy matrix, which is in good agreement with the result of XRD pattern. According to Fig.1b, the dendrite volume fraction is approximately 46.37%.

Fig.2 displays DSC curve of the as-cast $\text{Ti}_{48}\text{Zr}_{20}\text{Nb}_{12}\text{Cu}_5\text{Be}_{15}$ BMGC at a heating rate of 20 K/min. The T_g and T_x of the as-cast BMGC are marked in the curve as 633 and 725 K, respectively. It can also be noticed that there is a slight exothermic process before T_g (circle area in Fig.2), suggesting that a new crystalline phase may form before T_g of Ti-based BMGC.

2.2 Mechanical property of BMGC

The tensile property of $\text{Ti}_{48}\text{Zr}_{20}\text{Nb}_{12}\text{Cu}_5\text{Be}_{15}$ BMGC was

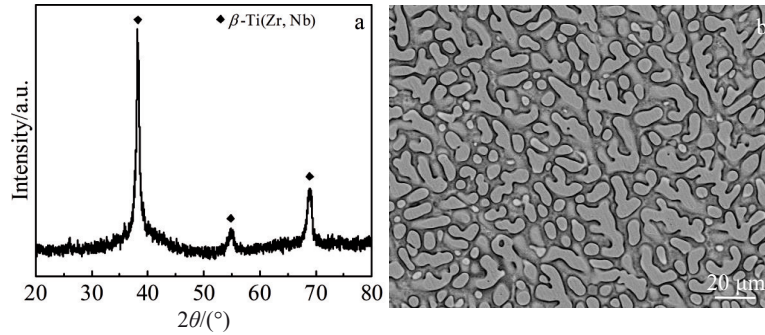


Fig.1 XRD pattern (a) and SEM image (b) of as-cast $\text{Ti}_{48}\text{Zr}_{20}\text{Nb}_{12}\text{Cu}_5\text{Be}_{15}$ metallic glass composite

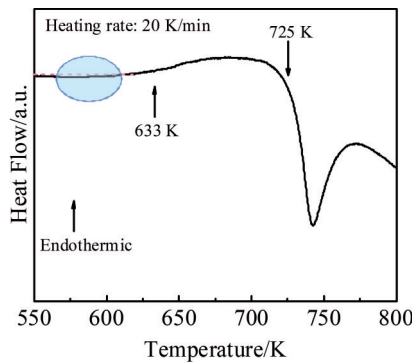


Fig.2 DSC curve of $\text{Ti}_{48}\text{Zr}_{20}\text{Nb}_{12}\text{Cu}_5\text{Be}_{15}$ metallic glass composite at heating rate of 20 K/min

measured at room temperature, and the stress-strain curve is exhibited in Fig.3. The tensile strength of $\text{Ti}_{48}\text{Zr}_{20}\text{Nb}_{12}\text{Cu}_5\text{Be}_{15}$ BMGC is about 1350 MPa, and the fracture strain is approximately 0.13. It can be seen that BMGC undergoes the work-hardening stage after yielding. Subsequently, the stress is decreased with increasing the strain due to the necking phenomenon before fracture, and the necking can be clearly observed from the fracture morphology, as shown in the inset of Fig.3. Thus, the great strength and plasticity during tensile deformation can be achieved.

2.3 Dynamic mechanical properties of BMGC

Dynamic mechanical properties of $\text{Ti}_{48}\text{Zr}_{20}\text{Nb}_{12}\text{Cu}_5\text{Be}_{15}$

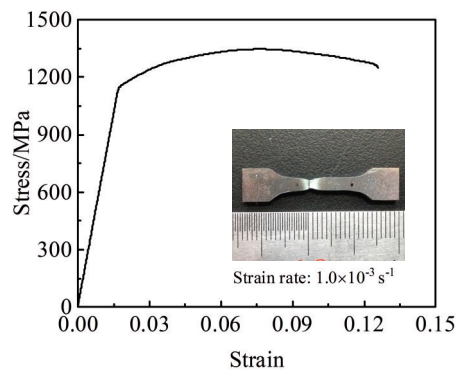


Fig.3 Tensile stress-strain curve of $\text{Ti}_{48}\text{Zr}_{20}\text{Nb}_{12}\text{Cu}_5\text{Be}_{15}$ metallic glass composite at room temperature

BMGC were analyzed through the storage modulus G' and loss modulus G'' . These moduli G' and G'' are normalized by unrelaxed modulus G_u , which is assumed to be equal to G' at room temperature. Then the normalized storage modulus G'/G_u and the normalized loss modulus G''/G_u are considered as a function of temperature under a fixed driving frequency of 0.3 Hz at a heating rate of 3 K/min, as shown in Fig.4. The typical dynamic mechanical behavior of $\text{Ti}_{48}\text{Zr}_{20}\text{Nb}_{12}\text{Cu}_5\text{Be}_{15}$ BMGC is similar to that of other BMGCs^[40] and BMGCs^[13,41]: three distinct temperature regions can be observed. Region I: at relatively low temperatures (from room temperature to about 627 K), both phases of BMGC are in solid state, so G' is high, G'' is very low, and they are almost constant, mainly indicating the elastic property in this region. Region II: at 627~820 K, the dynamic glass transition behavior of the amorphous matrix in BMGC appears. The temperature between T_g and T_x is the supercooled liquid region (SLR) of an amorphous material. In SLR, the amorphous matrix is in superplastic state, the β -Ti dendrites are still in solid state, and BMGC is mainly in viscoelastic state. Therefore, the G'' increases to its maximum value, and the corresponding temperature is T_α which is related to α relaxation or main relaxation of the amorphous matrix. The G' decreases to its minimum value almost at T_x . After that, the amorphous matrix begins to crystallize, leading to the decrease in G'' and the increase in G' . Region III: during the crystallization of the amorphous matrix, the G'' increases and the G' decreases. In this region, the crystallization of the amorphous matrix is finished and it is in solid state. However, the β -Ti softening temperature is

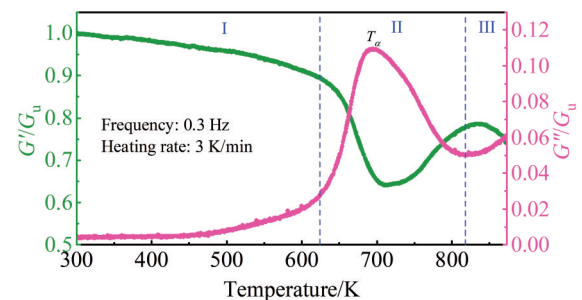


Fig.4 Normalized storage modulus G'/G_u and normalized loss modulus G''/G_u of as-cast $\text{Ti}_{48}\text{Zr}_{20}\text{Nb}_{12}\text{Cu}_5\text{Be}_{15}$ BMGC

achieved. Therefore, the loss modulus G'' is increased and the storage modulus G' is decreased slightly with increasing the temperature. However, the entire process is slightly different from the variation tendency of typical BMGs^[40], because of the existence of the secondary phase β -Ti dendrite. In SLR, even if the amorphous matrix is in the superplastic state, the secondary phase β -Ti dendrite still maintains the solid state, resulting in the fact that BMGC cannot be in semisolid state.

2.4 Theoretical analysis of dynamic mechanical behavior

To further understand the dynamic mechanical behavior of BMGC from the perspective of atomic motion, the quasi-point defects model^[42] was adopted. When an object receives an activation energy from the outside, the local movement can only occur in some weak regions, namely quasi-point defects^[43]. Palmer et al^[44] firstly proposed the framework of this model for metallic glasses. For metallic glasses, the motion of atoms or molecules is assisted by quasi-point defects and has a hierarchical correlation. The global characteristic time τ_{mol} is adopted to reflect the motion, and τ_{mol} is defined as the mean duration of a structural unit jumping over the distance of its own dimension, as expressed by Eq.(1) as follows:

$$\tau_{\text{mol}} = t_0 \left(\frac{\tau_{\beta}}{t_0} \right)^{\frac{1}{\chi}} \quad (1)$$

where t_0 is time scale parameter, τ_{β} is the mean time required for a structural unit jumping under thermal activation, and χ is correlation coefficient of 0~1. τ_{β} can be described by Arrhenius law, as follows:

$$\tau_{\beta} = \tau_0 \exp\left(\frac{E_a}{kT}\right) \quad (2)$$

where E_a is the activation energy required for the migration of a structural unit, τ_0 is pre-exponential time, T is the temperature, and k is the gas constant. The correlation coefficient χ corresponds to the quasi-point defect concentration. When $\chi = 0$, the atomic arrangement is in maximum order, corresponding to the perfect crystal, i.e., the movement of any structural unit requires the cooperative movement of all the other units. When $\chi = 1$, the atomic arrangement is in maximum disorder, corresponding to the perfect gas. It also means that the movement of any structural unit is independent of any other structural unit.

The loss factor can be expressed as follows:

$$\ln(\tan\delta) = \frac{E_a}{kT} - \chi \ln \omega - \chi \ln \tau^* + \lambda \quad (3)$$

$$\tau^* = t_0 \left(\frac{\tau_{\beta}}{t_0} \right)^{\frac{1}{\chi}} \quad (4)$$

where λ is a constant and ω is driving frequency.

The microstructure of amorphous material can remain frozen or isoconfigurational state when the temperature is below the glass transition temperature T_g , and the correlation coefficient χ is constant, presenting the Arrhenius behavior. In contrast, the metastable thermodynamic equilibrium occurs when the temperature is higher than glass transition temperature, and the correlation coefficient χ is increased with

increasing the temperature. Therefore, Eq. (5) and Eq. (6) can be obtained, as follows:

$$\chi(T) = \chi(T_g) \quad T < T_g \quad (5)$$

$$\chi(T) = \chi(T_g) + f(T) \quad T > T_g \quad (6)$$

At a fixed temperature, the corresponding activation energy E_a of a certain material is fixed, and the average time required for the transition of atoms or molecules in the material is also fixed. Thus, the first and third terms on the right side in Eq.(3) are constant at a fixed temperature. Then, the correlation coefficients at different temperatures can be obtained by measuring the values of $\ln(\tan\delta)$ and frequency ω at different temperatures. The relationship between $\ln(\tan\delta)$ and frequency ω at different temperatures of $\text{Ti}_{48}\text{Zr}_{20}\text{Nb}_{12}\text{Cu}_5\text{Be}_{15}$ BMGC is shown in Fig. 5, and all the data show a good fitting relationship with Eq.(3). It can be seen that all the correlation coefficients are basically the same when the temperature is below the glass transition temperature, which is in good agreement with the prediction of the model; the correlation coefficient value is about 0.297, which is similar to that of other BMGCs^[13], but lower than that of typical metallic glasses^[45]. It is well known that the atomic mobility of metallic glass is reduced by structural relaxation (annealing below glass transition temperature) or partial crystallization. Furthermore, the correlation coefficient χ can reflect the atomic mobility in amorphous material. Thus, when the temperature exceeds T_g , the correlation coefficient exhibits parabolic tendency. The relationship between correlation coefficient and temperature is shown in Fig. 6a: χ is increased slightly with increasing the temperature when the temperature approaches T_g ; when temperature $T > T_g$, χ is decreased sharply with increasing the temperature. The main reason is that the amorphous matrix is superplastic in SLR, and thus the atomic mobility increases when the temperature approaches T_g . However, the secondary phase dendrites reduce the atomic mobility of the whole BMGC due to the following reasons. Firstly, the volume fraction of dendrites in this BMGC is about 46%, and the net-like dendrites restrict the superplastic flow of the amorphous matrix. This restriction reduces the atomic fluidity of BMGC. Secondly, the existence of dendrites

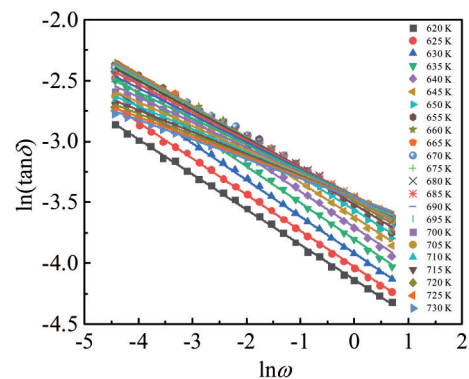


Fig.5 Relationship between loss factor $\tan\delta$ and driving frequency ω at different temperatures in $\text{Ti}_{48}\text{Zr}_{20}\text{Nb}_{12}\text{Cu}_5\text{Be}_{15}$ metallic glass composite (solid lines are fitting lines by Eq.(3))

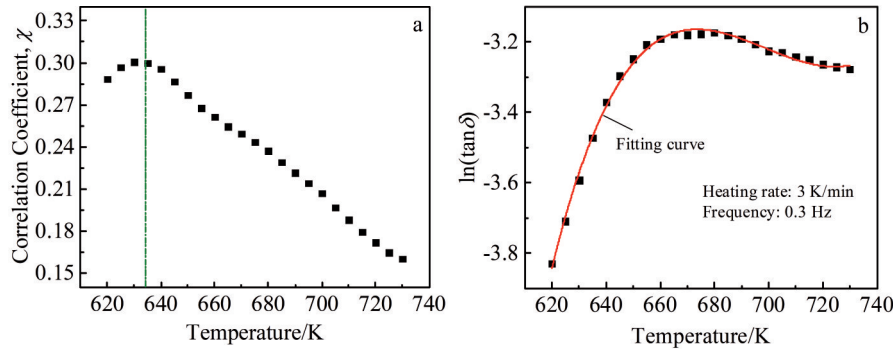


Fig.6 Evolution of correlation coefficient (a) and loss factor (b) with temperature of $\text{Ti}_{48}\text{Zr}_{20}\text{Nb}_{12}\text{Cu}_5\text{Be}_{15}$ BMGC

sharply reduces the thermostability of amorphous matrix, which is similar to the fact that annealing can generate the crystallization in BMG even if the temperature in SLR is below $T_x^{[46]}$. Even below the T_g , the formation of nanocrystalline nuclei in the amorphous matrix can also be observed in the Ti-based BMGC^[13]. Therefore, when temperature $T < T_g$, the correlation coefficient χ is increased with increasing the temperature; when temperature $T > T_g$, the correlation coefficient χ begins to decrease with increasing the temperature due to the formation of nanocrystalline nuclei in the amorphous matrix. With the steady rise of crystallization volume fraction in the amorphous matrix, the correlation coefficient χ is decreased sharply when temperature $T > T_g$.

Furthermore, the relationship between loss factor and temperature at a given frequency can also be obtained from Eq. (3). The correlation coefficient χ is a constant at room temperature and there is no atomic transition behavior under thermal activation, so the expression of loss factor can be presented as follows:

$$\ln(\tan \delta) = \frac{E_a}{kT} + C_1 \quad (7)$$

However, when the temperature approaches or becomes higher than the glass transition temperature, the temperature dependence of correlation coefficient χ should be considered. The relationship between correlation coefficient and temperature is shown in Fig. 6a. Therefore, the correlation coefficient χ can be expressed as a general quadratic function of temperature T : $\chi = \alpha'T + \beta'T^2 + C$. So the expression of loss factor at high temperature can be expressed as follows:

$$\ln(\tan \delta) = \frac{E_a}{kT} + \alpha'T + \beta'T^2 + C_2 \quad (8)$$

where C_i ($i=1, 2$) is the constant related to T_g , τ^* , and λ ; α' and β' are polynomial coefficients. Therefore, the experiment results in this work fit well by Eq.(7) and Eq.(8), as shown in Fig. 6b. The fitting curve is in good agreement with the experiment data points, indicating that quasi-point defects model can well describe the influence of temperature on the dynamic mechanical behavior of $\text{Ti}_{48}\text{Zr}_{20}\text{Nb}_{12}\text{Cu}_5\text{Be}_{15}$ BMGC.

3 Conclusions

1) The tensile strength of $\text{Ti}_{48}\text{Zr}_{20}\text{Nb}_{12}\text{Cu}_5\text{Be}_{15}$ bulk metallic glass composites (BMGCs) is about 1350 MPa, and the

fracture strain is approximately 0.13, which shows great strength and plasticity in $\text{Ti}_{48}\text{Zr}_{20}\text{Nb}_{12}\text{Cu}_5\text{Be}_{15}$ BMGC.

2) With increasing the temperature, the state of BMGC can be divided into three regions. Region I: when the temperature is less than 627 K, the state of BMGC is mainly elastic; Region II: when the temperature is 627~820 K, BMGC is mainly in viscoelastic state; Region III: due to the crystallization of amorphous matrix and the softening of dendrite, the loss modulus is increased and the storage modulus is decreased slightly.

3) When the temperature approaches the glass transition temperature T_g , the correlation coefficient χ is increased with increasing the temperature because the amorphous matrix is in superplastic state. When the temperature is over T_g , χ is decreased sharply due to the crystallization.

4) The loss factor has different functional relationships with the temperature. At room temperature, the loss factor has a linear relationship with the temperature. When the temperature approaches or becomes higher than the glass transition temperature, the loss factor has a quadratic function relationship with the temperature. The quasi-point defects model can well describe the influence of temperature on the dynamic mechanical behavior of $\text{Ti}_{48}\text{Zr}_{20}\text{Nb}_{12}\text{Cu}_5\text{Be}_{15}$ BMGC.

References

- Gilbert C J, Ritchie R O, Johnson W L. *Applied Physics Letters* [J], 1997, 71(4): 476
- Qiao J C, Yao Y, Pelletier J M et al. *International Journal of Plasticity*[J], 2016, 82: 62
- Yu W Q, Lu L P, Zuo B et al. *Rare Metal Materials and Engineering*[J], 2020, 49(5): 1561
- Chen J, Zhu Z H, Lin Q Y et al. *Rare Metal Materials and Engineering*[J], 2020, 49(4): 1204
- Qiao J C, Wang Q, Pelletier J M et al. *Progress in Materials Science*[J], 2019, 104: 250
- Hao Q, Qiao J C, Goncharova E V et al. *Chinese Physics B*[J], 2020, 29(8): 86 402
- Chen M W. *Annual Review of Materials Research*[J], 2008, 38: 14
- Hufnagel T C, Schuh C A, Falk M L. *Acta Materialia*[J], 2016, 109: 375

- 9 Zhang Y, Liu J P, Chen S Y et al. *Progress in Materials Science* [J], 2017, 90: 358
- 10 Greer A L, Cheng Y Q, Ma E. *Materials Sciences and Engineering R: Reports*[J], 2013, 74(4): 71
- 11 Zhao P Y, Li J, Wang Y Z. *International Journal of Plasticity*[J], 2013, 40: 1
- 12 Wang W H, Yang Y, Nieh T G et al. *Intermetallics*[J], 2015, 67: 81
- 13 Qiao J C, Sun B A, Gu J et al. *Journal of Alloys and Compounds* [J], 2017, 724: 921
- 14 Wang W H. *Progress in Materials Science*[J], 2012, 57(3): 487
- 15 Liu S T, Wang Z, Peng H L et al. *Scripta Materialia*[J], 2012, 67(1): 9
- 16 Lu Z, Jiao W, Wang W H et al. *Physical Review Letters*[J], 2014, 113(4): 4550
- 17 Wang Z, Sun B A, Bai H Y et al. *Nature Communications*[J], 2014, 5: 5823
- 18 Wang S, Ye Y F, Sun B A et al. *Journal of the Mechanics and Physics of Solids*[J], 2015, 77: 70
- 19 Wu Y, Wang H, Wu H H et al. *Acta Materialia*[J], 2011, 59(8): 2928
- 20 Jiang W H, Liu F X, Liaw P K. *Applied Physics Letters*[J], 2007, 90(18): 181 903
- 21 Schuh C A, Hufnagel T C, Ramamurty U. *Acta Materialia*[J], 2007, 55(12): 4067
- 22 Gao Y F, Wang L, Bei H et al. *Acta Materialia*[J], 2011, 59(10): 4159
- 23 Yang Y, Liu C T. *Journal of Materials Science*[J], 2012, 47(1): 55
- 24 Sun B A, Wang W H. *Progress in Materials Science*[J], 2015, 74: 211
- 25 Zhao J X, Wu F E, Qu R T et al. *Acta Materialia*[J], 2010, 58(16): 5420
- 26 Scudino S, Surreddi K B, Wang G et al. *Scripta Materialia*[J], 2010, 62(10): 750
- 27 Kawamura Y, Shibata T, Inoue A et al. *Scripta Materialia*[J], 1997, 37(4): 431
- 28 Kawamura Y, Nakamura T, Inoue A. *Scripta Materialia*[J], 1998, 39(3): 301
- 29 Jang D C, Greer J R. *Nature Materials*[J], 2010, 9(3): 215
- 30 Madge S V, Sharma P, Louzguine-Luzgin D V et al. *Scripta Materialia*[J], 2010, 62(4): 210
- 31 Sun B A, Song K K, Pauly S et al. *International Journal of Plasticity*[J], 2016, 85: 34
- 32 Qiao J W, Jia H L, Liaw P K. *Materials Sciences and Engineering R: Reports*[J], 2016, 100: 1
- 33 Ma Yunfei, Gong Pan, Li Fangwei et al. *Rare Metal Materials and Engineering*[J], 2020, 49(4): 1445 (in Chinese)
- 34 Wu F F, Chan K C, Jiang S S et al. *Scientific Reports*[J], 2014, 4(1): 5302
- 35 Wu Y, Ma D, Li Q K et al. *Acta Materialia*[J], 2017, 124: 478
- 36 Kolodziejska J A, Kozachkov H, Kranjc K et al. *Scientific Reports*[J], 2016, 6: 22 563
- 37 Zhang L, Pauly S, Tang M Q et al. *Scientific Reports*[J], 2016, 6: 19 235
- 38 Etienne S, Cavaille J Y, Perez J et al. *Review of Scientific Instruments*[J], 1982, 53(8): 1261
- 39 Pelletier J M, Gauthier C, Munch E. *Materials Sciences and Engineering A*[J], 2006, 442(1-2): 250
- 40 Qiao J C, Pelletier J M, Casalini R. *Journal of Physical Chemistry B*[J], 2013, 117(43): 13 658
- 41 Li J S, Cui J, Qiao J C et al. *Journal of Applied Physics*[J], 2015, 117(15): 155 102
- 42 Perez J, Cavaille J Y, Eienne S et al. *Annales de Physique*[J], 1983, 8: 417
- 43 Turnbull D, Cohen M H. *The Journal of Chemical Physics*[J] 1961, 34(1): 120
- 44 Palmer R G, Stein D L, Abrahams E et al. *Physical Review Letters*[J], 1984, 53(10): 958
- 45 Qiao J C, Pelletier J M, Esnouf C et al. *Journal of Alloys and Compounds*[J], 2014, 604: 139
- 46 Cui J, Li J S, Wang J et al. *Journal of Non-crystalline Solids*[J], 2014, 404: 7

Ti₄₈Zr₂₀Nb₁₂Cu₅Be₁₅非晶复合材料的内耗行为

崔晶¹, 柳翊², 刘抒¹

(1. 深圳职业技术学院 工业训练中心, 广东 深圳 518055)

(2. 洛阳理工学院 材料科学与工程学院, 河南 洛阳 471023)

摘要: 对Ti₄₈Zr₂₀Nb₁₂Cu₅Be₁₅非晶复合材料的室温力学性能以及随温度变化的动态力学性能进行了研究。结果表明, 该非晶复合材料的室温拉伸强度约为1350 MPa, 断裂应变约为0.13。随着温度的升高, 该非晶复合材料的整体状态由弹性转变为粘弹性。在准点缺陷模型框架下, 引入了诸如损耗因子、相关系数等相关物理参数, 全面分析了该非晶复合材料动态力学行为, 并且模型的理论曲线与实验数据拟合程度较好。因此, 准点缺陷模型可以很好地描述不同温度下的Ti₄₈Zr₂₀Nb₁₂Cu₅Be₁₅非晶复合材料的动态力学行为。

关键词: 非晶复合材料; 机械性能; 动态力学行为; 准点缺陷

作者简介: 崔晶, 男, 1983年生, 博士, 深圳职业技术学院工业训练中心, 广东 深圳 518055, E-mail: cuijing@szpt.edu.cn